



TITLE:

# Synthesis of trans-1,2-dimetalloalkenes through reductive anti-dimagnesiumation and dialumination of alkynes

AUTHOR(S):

Takahashi, Fumiya; Kurogi, Takashi; Yorimitsu, Hideki

---

CITATION:

Takahashi, Fumiya ...[et al]. Synthesis of trans-1,2-dimetalloalkenes through reductive anti-dimagnesiumation and dialumination of alkynes. *Nature Synthesis* 2023, 2(2): 162-171

ISSUE DATE:

2023-02

URL:

<http://hdl.handle.net/2433/279263>

RIGHT:

© The Author(s) 2023; This article is licensed under a Creative Commons Attribution 4.0 International License, which permits use, sharing, adaptation, distribution and reproduction in any medium or format, as long as you give appropriate credit to the original author(s) and the source, provide a link to the Creative Commons license, and indicate if changes were made. The images or other third party material in this article are included in the article's Creative Commons license, unless indicated otherwise in a credit line to the material. If material is not included in the article's Creative Commons license and your intended use is not permitted by statutory regulation or exceeds the permitted use, you will need to obtain permission directly from the copyright holder.



# Synthesis of *trans*-1,2-dimetalloalkenes through reductive *anti*-dimagnesiumation and dialumination of alkynes

Received: 19 May 2022

Accepted: 12 October 2022

Published online: 2 January 2023

 Check for updates

 Fumiya Takahashi , Takashi Kurogi & Hideki Yorimitsu  

Polar reactive organometallic species have been key reagents in synthesis for more than a century. Stereodefined 1,2-dimetalated alkenes offer promising synthetic utility; however, few methods are available for their preparation due to their relatively low stability. Here we report the reductive *anti*-1,2-dimetalation of alkynes to stereoselectively generate *trans*-1,2-dimagnesio- and 1,2-dialuminoalkenes, which are stable and have been demonstrated in organic synthesis. These stereodefined 1,2-dimetalated alkenes are prepared through the use of a sodium dispersion as a reducing agent, and organomagnesium and organoaluminium halides as reduction-resistant electrophiles. Highly nucleophilic 1,2-dimagnesioalkenes serve as dual Grignard reagents and have been demonstrated to react with various electrophiles to afford *anti*-difunctionalized alkenes. The 1,2-dialuminoalkenes react with paraformaldehyde with dearomatization of the aryl moieties to form the corresponding dearomatized 1,4-diols, with the overall reaction being regarded as alkynyl-directed dearomatization of arenes. X-ray crystallographic analysis further supports the formation of *trans*-1,2-dimagnesio- and 1,2-dialuminoalkenes, with computational studies providing insight into the mechanism of dearomative difunctionalization.

Organometallic species bearing a polar carbon–metal bond occupy an indispensable position in organic chemistry due to their high reactivity<sup>1</sup>. As a representative organomagnesium species, Grignard reagents have been widely used for the synthesis of useful molecules ranging from bioactive compounds to organic semiconductors since their discovery in 1900<sup>2,3</sup>. Nowadays, a variety of polar organometallic species, such as organolithium, organozinc and organoaluminium compounds, are readily available and have significantly contributed to the development of organic chemistry.

The preparation of such polar organometallics is often dependent on deprotonation at acidic C–H bonds or on metallation of organic halides via a reductive process or halogen–metal exchange (Fig. 1a)<sup>4–6</sup>. Although these methods are reliable, special classes of precursors, acidic hydrocarbons and halogenated compounds are necessary.

Unsaturated hydrocarbons such as alkenes and alkynes represent another important class of precursor (Fig. 1b). Hydrometallation and carbometallation across unsaturated bonds provide highly useful reactive organometallic species such as alkyl and alkenyl metals<sup>7–12</sup>. A key advantage of metallating unsaturated bonds is the increase in molecular complexity and values by starting from simple unsaturated compounds such as alkynes, which are among the most prevalent and primitive structures in organic molecules. The subsequent conversion of the resulting carbon–metal bond then offers straightforward routes to target molecules.

Given the unparalleled importance of monometallation such as hydrometallation and carbometallation, 1,2-dimetalation of unsaturated bonds would be a fascinating transformation. For example, two-electron reduction of alkynes should ideally lead to 1,2-dimetalation

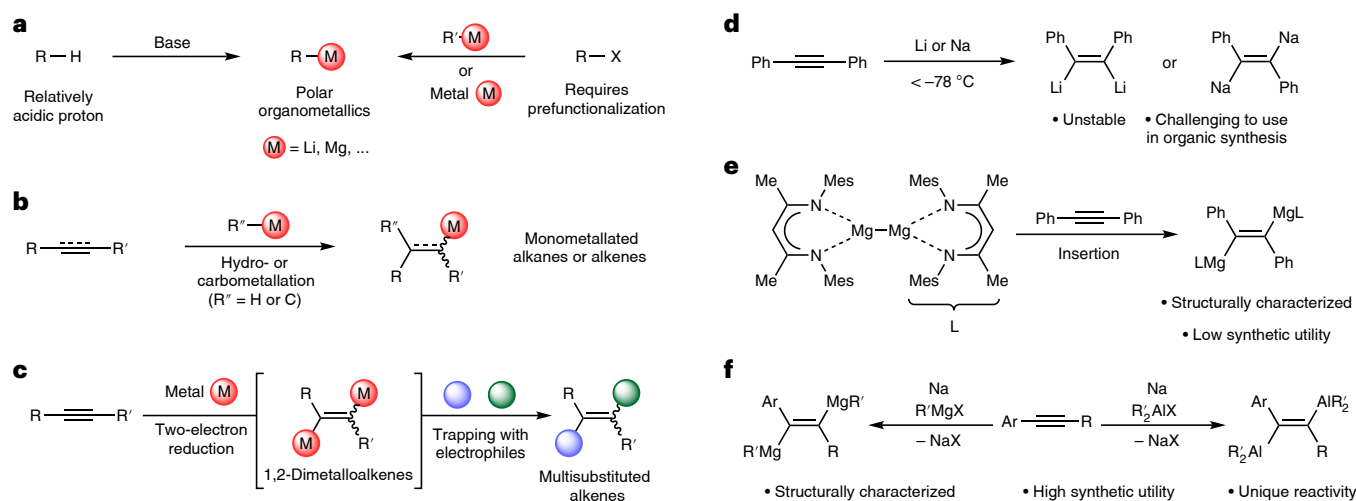


**Fig. 1 | Generation of 1,2-dimetalloalkenes.** **a**, Generation of polar organometallic species by deprotonation of relatively acidic protons from hydrocarbons (left) and halogen–metal exchange or reductive metallation of organic halides (right). **b**, Hydrometallation and carbometallation of unsaturated compounds provide the corresponding monometallated polar organometallics. **c**, 1,2-Dimetalloalkenes generated by two-electron reduction of alkynes can act as versatile precursors for multisubstituted alkenes. **d**, 1,2-Dilithio- and 1,2-disodioalkenes are too unstable to be utilized as synthetic intermediates<sup>13</sup>.

**e**, There is only one example of an isolated monomeric 1,2-dimagnesiumalkene reported by Jones et al.<sup>14</sup>. However, the synthetic utility of the species has not yet been fully demonstrated. Mes, 2,4,6-trimethylphenyl. **f**, The present work: developing a method for 1,2-dimagnesiumation and 1,2-dialuminumation of alkynes. The generated 1,2-dimetalloalkenes are isolated and structurally characterized. 1,2-Dimagnesiumalkenes work as ‘1,2-bis(Grignard)’ reagents towards various electrophiles to provide multisubstituted alkenes. 1,2-Dialumino-1-arylalkenes react with aldehydes accompanied by dearomatization of the aryl moiety.

(Fig. 1c). The resulting 1,2-dimetalloalkenes should engage in further bond formations at the two reactive carbon–metal bonds to provide a wide variety of multisubstituted alkenes that are otherwise difficult to synthesize. Despite this promising utility, few methods for generating polar reactive 1,2-dimetalloalkenes have been reported<sup>13–18</sup>. The limited research is considered to be due to the following reactivity–stability trade-off issues. (1) Electron injection into alkynes requires strong reductants such as alkali metals and solvated electrons. (2) After electron injection from alkali metal occurs, the resulting radical anion intermediates and the 1,2-dimetalloalkene products are too unstable for use in organic synthesis. When the electron injection to alkynes is too slow, as in the reduction of diphenylacetylene with lithium in Et<sub>2</sub>O, the generated radical anion intermediates readily dimerize to form 1,4-dimetallo-1,3-butadienes<sup>19,20</sup>. While 1,2-dilithio- and 1,2-disodioalkenes can be generated from diphenylacetylene and alkali metal in THF<sup>13</sup>, they decompose via protonation by the THF solvent even at –78 °C and cannot be used for organic synthesis (Fig. 1d). Another notable example is that the dissolving metal reduction of alkynes always ends up with the formation of *trans*-alkenes via smooth protonations of anionic intermediates by a protic solvent (liquid ammonia) with isolation of any vinylic metal intermediates being elusive. (3) As examples of very limited successful cases, engineered bulky dinuclear Mg(I) and Al(II) complexes<sup>14–16</sup> are known to undergo *anti*-dimetallation and yield stable *trans*-1,2-dimetalloalkenes (Fig. 1e). Bulky diiminatoaluminium chloride complexes are also known to undergo *anti*-dialuminumation in the presence of potassium metal via the addition of an aluminium-centred radical to alkynes<sup>17,18</sup>. However, these complexes are ingeniously designed and decorated with special ligands, and are thus not readily accessible. Furthermore, the generated 1,2-dimetalloalkenes were not used for organic synthesis but were examined to undergo simple protonolysis, iodolysis and transmetalation to zinc. (4) While a different approach to 1,2-dimetalloalkenes could be dimetallation of 1,2-dihaloalkenes, β-elimination from the 1-metallo-2-haloalkene intermediates takes place more rapidly than the second metallation<sup>21–23</sup>. Therefore, there remains ample room to develop facile synthesis and applications of potentially useful 1,2-dimetalloalkenes.

We have been interested in the development of alkali-metal-promoted reductive transformation of unsaturated compounds<sup>24–28</sup> using reduction-resistant electrophiles as key reagents<sup>29–31</sup>. On one hand, this class of electrophiles, which includes trialkoxyboranes, are resistant to single-electron reduction and hence can coexist in the same pot where the reduction of unsaturated substrates takes place. On the other hand, they are sufficiently electrophilic to immediately trap the unstable anions thus formed. We have developed sodium-mediated 1,2-*syn*-diboration of alkynes with trimethoxyborane<sup>30</sup>. This success encouraged us to develop a new method to generate more reactive and polar 1,2-dimetalloalkenes that are much more difficult to prepare and use. Here we report that the sodium-mediated reductive dimetallation of alkynes proceeds in the presence of magnesium- and aluminium-based reduction-resistant electrophiles (Fig. 1f). The reaction efficiently affords the corresponding reactive but stable 1,2-dimetalloalkenes with, more importantly, high *anti*-selectivity that is hard to achieve. The resulting *trans*-1,2-dimagnesiumalkenes react with various electrophiles to afford the corresponding *trans*-difunctionalized alkenes. Their aluminium equivalents were found to induce an unexpected dearomatization<sup>32–38</sup> at the terminal arene upon treatment with an aldehyde. Crystallographic analysis of the intermediates and density functional theory (DFT) calculations of the dearomatization are also described herein.

## Results and discussion

### Optimization and reaction scope of dimagnesiumation

We started our investigation by optimizing the reaction conditions for 1,2-dimagnesiumation of diphenylacetylene (**1a**) (Table 1). The corresponding organomagnesium species **2a** should be sensitive to air and moisture, and burdensome to isolate; therefore, the reaction efficiency was evaluated by the yield of stable diborylated product **3a** after treatment of **2a** with a boron electrophile. Following the conditions of the diboration of alkynes<sup>30</sup>, we initially employed magnesium alkoxides and halides as reduction-resistant magnesium electrophiles. However, magnesium ethoxide and related alkoxides were not readily soluble in THF, so that **3a** was not obtained at all. Magnesium dichloride was not resistant to reduction and underwent preferential reduction to Rieke-type magnesium<sup>39</sup> without forming **3a**. After further trials, it was

**Table 1 | Screening conditions for dimagnesiation of diphenylacetylene (**1a**)**

Entry	Mg reagent <sup>a</sup>	Alkali metal	B electrophile	NMR yield <sup>b</sup> (E:Z)
1 <sup>c</sup>	<sup>t</sup> PrMgBr	Na dispersion	MeOBpin	90% (57:43)
2 <sup>c</sup>	<sup>t</sup> PrMgBr	Na dispersion	EtOBpin	86% (78:22)
3	<sup>t</sup> PrMgBr	Na dispersion	<sup>i</sup> PrOBpin	75% (80:20)
4	MeMgBr	Na dispersion	<sup>i</sup> PrOBpin	49% (47:53)
5	<sup>t</sup> BuMgCl	Na dispersion	<sup>i</sup> PrOBpin	75% (72:28)
6	PhMgBr	Na dispersion	<sup>i</sup> PrOBpin	71% (41:59)
7	<sup>o</sup> PentMgBr	Na dispersion	<sup>i</sup> PrOBpin	85% (88:12)
8	<sup>o</sup> PentMgBr	Na lump	<sup>i</sup> PrOBpin	25% (76:24)
9	<sup>o</sup> PentMgBr	Li granule	<sup>i</sup> PrOBpin	14% (36:64)
10	<sup>o</sup> PentMgBr	Li powder	<sup>i</sup> PrOBpin	59% (51:49)
11	<sup>o</sup> PentMgBr	NaC <sub>10</sub> H <sub>8</sub>	<sup>i</sup> PrOBpin	74% (91:9)

<sup>a</sup>Magnesium reagents were used as a THF solution (~1M). <sup>b</sup>Yields were determined using <sup>1</sup>H NMR spectroscopy with dibromomethane as an internal standard. <sup>c</sup>The borylation step was conducted for 1 h. pin, pinacol.

discovered that the Grignard reagents are suitable reduction-resistant magnesium electrophiles in the presence of alkynes although they are always considered as nucleophiles in organic synthesis.

In the presence of 2 equiv. of isopropylmagnesium bromide, **1a** was reduced by 2 equiv. of a sodium dispersion (in mineral oil) in THF at 0 °C before treatment with methoxy-pinacolborane (MeOBpin) at 60 °C for 1 h (entry 1). The expected dimagnesiation and diborylation proceeded to afford **3a** in 90% yield, although without stereoselectivity. Other boron electrophiles such as ethoxy-pinacolborane (EtOBpin) and isopropoxy-pinacolborane (<sup>i</sup>PrOBpin) were screened, which identified <sup>i</sup>PrOBpin as the best for stereoretentive diboration (entries 2 and 3). The effect of the substituent on the organomagnesium species was investigated next. When methylmagnesium bromide (MeMgBr) was used, the conversion of **1a** was relatively low, possibly because the reduction of MeMgBr competed with that of **1a** (entry 4). The use of *tert*-butylmagnesium bromide or phenylmagnesium bromide afforded **3a** with low stereoselectivities, although with good yields (entries 5 and 6). Finally, cyclopentylmagnesium bromide (<sup>o</sup>PentMgBr) was found to be optimal in terms of both yield and selectivity (entry 7). When sodium lumps (diameter, ~2 mm) or lithium granules (diameter, ~2 mm) were used as the reductant, the efficiency of the electron transfer was so low because of their small surface area that the conversion of **1a** was insufficient (entries 8 and 9). The use of lithium powder (diameter, ~0.12–0.25 mm) improved the yield of **3a** to 59%, although a lower yield than that in entry 7 (entry 10). Employing sodium naphthalenide resulted in the formation of **3a** in 74% yield with good stereoselectivity (entry 11).

Having optimized reaction conditions (Table 1, entry 7), we investigated the scope of this dimagnesiation–diborylation sequence with respect to diarylacetylenes (Fig. 2a). It is worth noting that yields of the pure *E* isomers of **3** are shown here since the major isomers (*E*)-**3** could be easily separated from the minor isomers (*Z*)-**3** (*E*:*Z* = 77:23–91:9) by means of routine silica-gel chromatography (see Supplementary Information for the yields and isomeric ratios of the products in crude reaction mixtures). A variety of diarylacetylenes underwent the

reduction to yield the corresponding (*E*)-diborylalkenes **3a–j** in high yields, which represents a rare example of formal *anti*-diboration of alkynes<sup>40–44</sup>. In spite of the strongly reducing and basic conditions, ether (**3c** and **3f**), thioether (**3d**), fluoro (**3f**) and silyl (**3g**) moieties were well tolerated during the reaction. Moreover, sterically demanding *ortho*-substituents in diarylacetylenes **1i** and **1j** did not hamper the reaction. In addition, the present *anti*-diboration also accommodates arylacetylene with a  $\pi$ -extended naphthyl group (**1h**). Instead of boron electrophiles, carbonyl compounds such as paraformaldehyde reacted with **2** to yield 1,4-diols **4aa** and **4fa** in high yields (Fig. 2b).

To our delight, 1,2-dimagnesioalkenes **2** reacted with other electrophiles with the aid of a copper catalyst (Fig. 2c). CuCN·2LiCl (ref.<sup>45</sup>) catalysed the reaction of **2** with isobutylene oxide to provide the corresponding 1,6-diols **4ab**, **4eb** and **4kb** with complete *E*-selectivity, where none of the *Z* isomers were detected in crude reaction mixtures. Copper-catalysed reactions with methoxymethyl chloride and with allyl chloride similarly gave (*E*)-1,4-diether **4ac** and **4lc** and (*E*)-1,4,7-octatrienes **4ad** and **4fd** with exclusive stereoselectivity. Not only diarylacetylenes but alkylarylacetylene **1l** was also applicable to the present reaction. Moreover, the sequential addition of two different electrophiles to 1,2-dimagnesioalkenes **2** catalysed by copper accomplished unsymmetric 1,2-difunctionalizations. The desired unsymmetrically difunctionalized product **4ae** was obtained from symmetric diphenylacetylene (**1a**), and a differently tetrasubstituted alkene **4ie** was obtained via the regio- and stereoselective unsymmetric 1,2-difunctionalization of unsymmetric alkyne **1i**.

### Dialumination and subsequent dearomatization reaction

Encouraged by the success of the dimagnesiation, dialumination was attempted using an aluminium-based electrophile. When dimethylaluminium chloride was used as the electrophile, similar *anti*-dimetallation took place (Fig. 3a). Surprisingly, the subsequent reaction of the dialuminoalkene **5a** with paraformaldehyde resulted in the formation of not **4aa** but an unexpected product, dearomatized diol **6a**, with regeneration of the alkyne unit and with exclusive anti-selectivity. Further optimization (Supplementary Table 2) of the conditions for the dialumination (in 4-methyltetrahydropyran (4-MeTHP) at –78 °C), as shown in Fig. 3b, afforded **6a** in 86% yield without the formation of **4aa** and its stereoisomer **4aa'**.

With the optimal conditions established, the scope with respect to arylacetylenes was explored (Fig. 3b). Diarylacetylenes **1a**, **1b**, **1h** and **1m** underwent the dearomatization to afford the corresponding 1,4-diols **6** in good yields. The naphthyl moiety of **1h** was selectively dearomatized, probably due to its lower aromaticity than that of the phenyl moiety. It is noteworthy that sterically demanding **1m** participated in the reaction to give a mixture of two regioisomers **6m** and **6m'**, regardless of the *ortho*-methyl substituent. The reaction also accommodates alkylarylacetylenes **1l** and **1n–p**. Biphenyl substrate **1o** reacted selectively on the phenyl ring with an alkynyl substituent to yield **6o**. Arylsilylacetylenes **1q** and **1r** were converted while the frangible silyl groups were untouched. These transformations are regarded as a novel class of dearomatization reaction of arylacetylenes directed by a carbon–carbon triple bond. As an additional note, these are rare examples of alkyne-directed reactions with the alkyne unit left in the products, while reported transformations directed by a carbon–carbon triple bond have always accompanied irreversible conversions of the reactive triple bond into a double bond<sup>46,47</sup>.

The obtained dearomatized 1,4-diol **6a** could be further transformed into complex molecules that would otherwise be difficult to synthesize (Fig. 3c). The Diels–Alder reaction with *N*-methylmaleimide or 4-phenyl-1,2,4-triazoline-3,5-dione gave the corresponding bicyclo[2.2.2]octene **7** or **8** in excellent yield as a single isomer. Gold-catalysed cycloisomerization of **6a** proceeded efficiently to form a tricyclic acetal **9** (ref.<sup>48</sup>). Oxidation of the diene moiety by photosensitized singlet oxygen followed by treatment with thiourea and acetylation





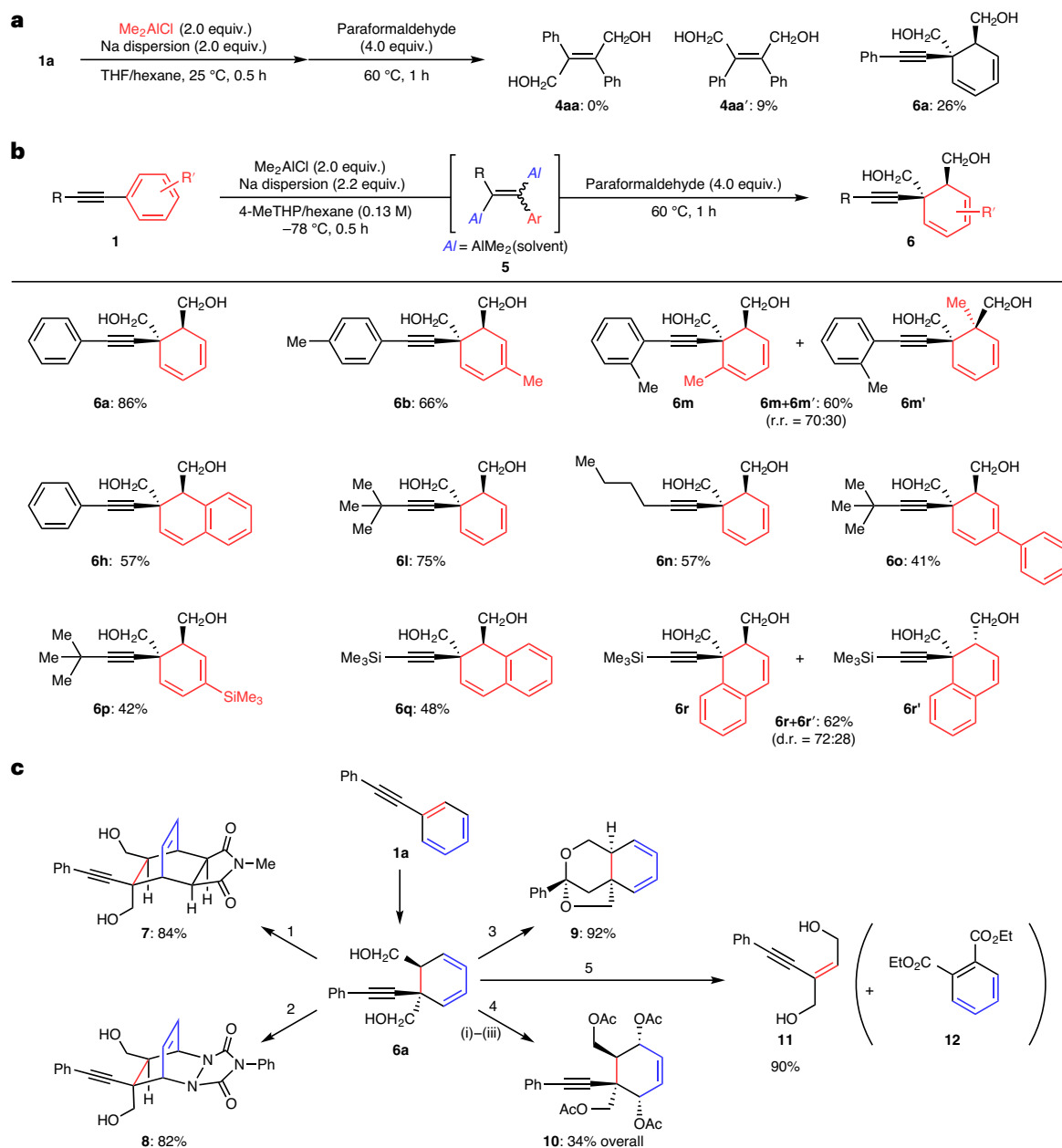


**Fig. 3 | Dearomative functionalization of arylacetylenes via**

**1,2-dialuminum.** **a**, The use of dimethylaluminium chloride instead of Grignard reagents resulted in 1,2-dialumination of diphenylacetylene. However, the resulting 1,2-dialuminoalkene reacted with paraformaldehyde at 60 °C (see below) unexpectedly to afford a dearomatized 1,4-diol **6a**. **b**, Various arylacetylenes underwent the aluminium-mediated dearomatizative functionalization. r.r., regioisomeric ratio; d.r., diastereomeric ratio. **c**, Derivatizations of dearomatized 1,4-diol **6a** under the following reaction

conditions: (1) **6a** (1.0 equiv.), *N*-methylmaleimide (1.5 equiv.), toluene, 60 °C, 38 h; (2) **6a** (1.0 equiv.), 4-phenyl-1,2,4-triazoline-3,5-dione (1.1 equiv.), THF, -78 °C, 1 h; (3) **6a** (1.0 equiv.), AuCl(PPh<sub>3</sub>) (2.5 mol%), AgOTf (2.5 mol%), *p*-TsOH·H<sub>2</sub>O (10 mol%), CH<sub>2</sub>Cl<sub>2</sub>, r.t., 1 h; (4) (i) **6a** (1.0 equiv.), Rose Bengal (1 mol%), air, ultraviolet irradiation, CH<sub>2</sub>Cl<sub>2</sub>, r.t., 3.5 h; (ii) thiourea (1.2 equiv.), MeOH, r.t., 13 h; (iii) Ac<sub>2</sub>O, pyridine, r.t., 3 h; (5) **6a** (1.0 equiv.), diethyl acetylenedicarboxylate (1.5 equiv.), neat, 100 °C, 21 h. Tf, trifluoromethanesulfonyl; Ts, *p*-toluenesulfonyl; Ac, acetyl

of NaCl, recrystallization from toluene provided the corresponding *trans*-1,2-dimagnesiumoethene **2a**<sup>iPr</sup>(THF)<sub>4</sub> as yellowish orange crystals in 47% yield. Following a similar procedure, *trans*-1,2-dialuminoethene **5a**<sup>Et</sup>(THF)<sub>2</sub> was prepared from diethylaluminium chloride as pale yellow crystals in 12% yield. The verification of the *trans* stereochemistry of **5** is important to eliminate the possibility of the preferential formation of its *cis* isomer<sup>51</sup>. X-ray diffraction analysis of single crystals of both **2a**<sup>iPr</sup>(THF)<sub>4</sub> and **5a**<sup>Et</sup>(THF)<sub>2</sub> displayed dimetallic structures where the two metals occupy the *trans*-positions to each other in the central ethene skeletons. The Cl–Cl' bonds in the [PhCCPh] unit

delivered from diphenylacetylene are elongated to typical C=C double bonds (1.328(6) Å for **2a**<sup>iPr</sup>(THF)<sub>4</sub> and 1.355(2) Å for **5a**<sup>Et</sup>(THF)<sub>2</sub>) along with formation of comparable C(sp<sup>2</sup>)–metal bonds (C1–Mg1 in **2a**<sup>iPr</sup>, 2.195(4) Å; C1–Al1 in **5a**<sup>Et</sup>, 2.005(2) Å) to those in the reported 1,2-dimagnesiumoethene<sup>14</sup> and 1,2-dialuminoethenes<sup>15–17</sup>. Akin to the C<sub>i</sub> symmetric system in the crystal structures, NMR spectral analysis of **2a**<sup>iPr</sup>(THF)<sub>4</sub> and **5a**<sup>Et</sup>(THF)<sub>2</sub> also revealed symmetric features in solution. Notably, the <sup>13</sup>C NMR spectra of **2a**<sup>iPr</sup>(THF)<sub>4</sub> and **5a**<sup>Et</sup>(THF)<sub>2</sub> showed highly downfield-shifted <sup>13</sup>C NMR resonances at 195.9 ppm and 175.9 ppm, respectively, compared with that of free diphenylacetylene,

while the phenyl rings of **2a**<sup>iPr</sup>(THF)<sub>4</sub> and **5a**<sup>Et</sup>(THF)<sub>2</sub> were observed in the typical aromatic region.

Having the isolated 1,2-dimetalloethenes **2a**<sup>iPr</sup>(THF)<sub>4</sub> and **5a**<sup>Et</sup>(THF)<sub>2</sub> in hand, we resorted to demonstrating reactivity similar to that shown in Figs. 2c and 3b. 1,2-Dimagnesioethene **2a**<sup>iPr</sup>(THF)<sub>4</sub> underwent the copper-catalysed hydroxyalkylation using isobutylene oxide to afford **4ab** in 80% yield (Supplementary Fig. 4a). 1,2-Dialuminoethene **5a**<sup>Et</sup>(THF)<sub>2</sub> reacted with paraformaldehyde to provide **6a** in 80% yield (Supplementary Fig. 4b).

### Computational investigation of dearomatization

To investigate the mechanism of the unique dearomatization of arylacetylenes (Fig. 3a,b), DFT calculations were performed using the reaction of 1,2-dialumino-1,2-diphenylethene **5a**<sup>Me</sup> with monomeric formaldehyde in THF solvent as a model reaction (Fig. 5).

In the case of dearomatization (Fig. 5a), the reaction begins with the coordination of a formaldehyde molecule to one of the aluminium atoms of **5a**<sup>Me</sup> to form metastable intermediate **INT-d1**<sub>tAl</sub>. The subsequent C–C bond formation with dearomatization of the neighbouring phenyl ring occurs via a six-membered cyclic transition state **TS-d1**<sub>tAl</sub> to provide a transient allenyl intermediate **INT-d2**<sub>tAl</sub>. Barrierless recoordination of a THF molecule to the tricoordinated aluminium atom gives a stable intermediate **INT-d3**<sub>tAl</sub>. The subsequent ligand exchange of THF with formaldehyde at the other aluminium atom affords **INT-d4**<sub>tAl</sub> before the second C–C bond formation proceeds again through a six-membered cyclic transition state **TS-d2**<sub>tAl</sub>. Favourable recoordination of a THF solvent molecule to the aluminium atom yields a dearomatized 1,4-diolate **INT-d5**<sub>tAl</sub> as the final product. The first C–C bond-forming step via **TS-d1**<sub>tAl</sub> with dearomatization is rate-determining ( $\Delta G^\ddagger = 18.8 \text{ kcal mol}^{-1}$ ) while the second C–C bond-forming step proceeds more smoothly ( $\Delta G^\ddagger = 8.3 \text{ kcal mol}^{-1}$ ), which is consistent with the experimental result that the allenyl by-products derived from **INT-d3**<sub>tAl</sub> were not observed at all. Benzylic metal species, especially benzylmagnesiums, are known to undergo nucleophilic addition to aldehyde with dearomatization despite low efficiency and regioselectivity<sup>52,53</sup>. Our reaction is much more efficient and regioselective, probably because the second nucleophilic attack drives the reaction forward and suppresses the collapse back to the original dialuminoalkene **5a**<sup>Me</sup> and formaldehyde. The low activation energy for each step allows the entire process to proceed smoothly even at room temperature. Although the reaction between **5** and paraformaldehyde was performed at 60 °C, high temperature is necessary for the decomposition of paraformaldehyde to the monomeric species H<sub>2</sub>C=O (Fig. 3b).

In the case of the conceivable twofold *ipso*-alkylation (Fig. 5b), the first and second C–C bond formations occur via four-membered cyclic transition states **TS-i1**<sub>tAl</sub> and **TS-i2**<sub>tAl</sub>, respectively. Unlike the dearomatization in Fig. 5a, the rate-determining step is the second C–C bond-forming step (**INT-i3**<sub>tAl</sub> → **TS-i2**<sub>tAl</sub>;  $\Delta G^\ddagger = 22.0 \text{ kcal mol}^{-1}$  versus 21.3 kcal mol<sup>-1</sup> for the first step), which is in good agreement with the experimental fact that a trace amount of monohydroxymethylated alkene derived from **INT-i3**<sub>tAl</sub> was observed as a side product. The difference between the activation energies for the first steps in Fig. 5a,b was calculated to be 2.6 kcal mol<sup>-1</sup> (18.8 kcal mol versus 21.3 kcal mol<sup>-1</sup>) in favour of the dearomatization process.

Similar calculations for the reaction of the magnesium counterpart **2a**<sup>Me</sup> with two molecules of formaldehyde were next conducted to identify similar pathways for the dearomatization and the twofold *ipso*-hydroxymethylations (Supplementary Figs. 7 and 8). In contrast to the aluminium case, the activation barrier of the first C–C bond formation step for the *ipso*-hydroxymethylation is much lower than that for the dearomatization ( $\Delta\Delta G^\ddagger = 7.6 \text{ kcal mol}^{-1}$ ), which coincides with the exclusive *ipso*-hydroxymethylation without the dearomatization as shown in Fig. 2b. Based on distortion/interaction analyses<sup>54,55</sup> (Supplementary Figs. 15–17), we assume that the shorter C–Al bond (2.08 Å) in **TS-i1**<sub>tAl</sub>

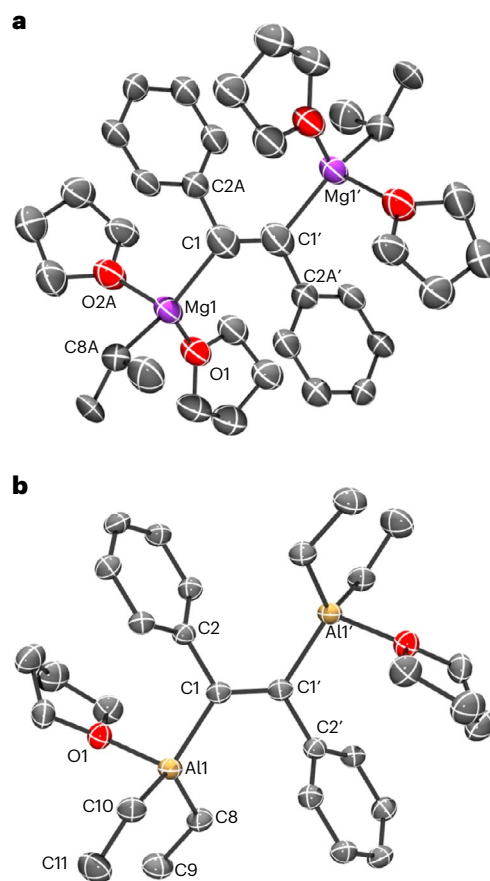


**Fig. 4 | Molecular structures of 1,2-dimetalloethenes.** Thermal ellipsoids are drawn at 50% probability. All of the hydrogen atoms are omitted for clarity. One part of the disordered moieties in **2a**<sup>iPr</sup>(THF)<sub>4</sub> is shown. **a**, Selected bond distances (Å) and angles (deg) of **2a**<sup>iPr</sup>(THF)<sub>4</sub>: C1–C1', 1.328(8); C1–C2A, 1.544(6); Mg1–C1, 2.195(4); Mg1–C8A, 2.173(10); C2A–C1–C1', 113.4(5); Mg1–C1–C2A, 115.9(4); Mg1–C1–C1', 130.7(5); C1–Mg1–C8A, 128.0(3). **b**, Selected bond distances (Å) and angles (deg) of **5a**<sup>Et</sup>(THF)<sub>2</sub>: C1–C1', 1.355(2); C1–C2, 1.498(3); Al1–C1, 2.005(2); Al1–C8, 1.984(2); Al1–C10, 2.009(2); C2–C1–C1', 117.8(2); Al1–C1–C2, 117.2(1); Al1–C1–C1', 124.9(2); C1–Al1–C8, 116.24(8); C8–Al1–C10, 118.07(9).

would induce a larger ring strain in the four-membered transition state **TS-i1**<sub>tAl</sub> than the C–Mg bond (2.22 Å) in **TS-i1**<sub>tMg</sub>, and consequently render the activation energy at **TS-i1**<sub>tAl</sub> higher.

### Conclusion

We have uncovered reductive *anti*-1,2-dimetallation of arylacetylenes using sodium dispersion as a reducing agent and cyclopentylmagnesium bromide and dimethylaluminium chloride as reduction-resistant electrophiles. The intermediates, *trans*-1,2-dimagnesio- and dialuminoalkenes, represent rare examples of *trans*-1,2-dimetalloalkenes that are difficult to prepare, reasonably stable and useful for organic synthesis. Highly nucleophilic 1,2-dimagnesioalkenes reacted with a wide variety of electrophiles to afford *anti*-difunctionalized alkenes in a stereoselective manner. Interestingly, the reaction of the 1,2-dialuminoalkenes with paraformaldehyde induced dearomatization of the aryl moieties to form the corresponding dearomatized 1,4-diols with recovery of the alkyne unit, which is regarded as alkynyl-directed dearomatization of arenes. These represent the synthetic versatility of the dimagnesioalkenes and the unique reactivity of the dialuminoalkenes. The structures of 1,2-dimagnesio- and dialuminoalkenes were unambiguously determined by X-ray crystallography to confirm their intermediacy. The mechanism of the dearomative difunctionalization was investigated using DFT calculations to clarify the unusual behaviour of unique organoaluminium species.

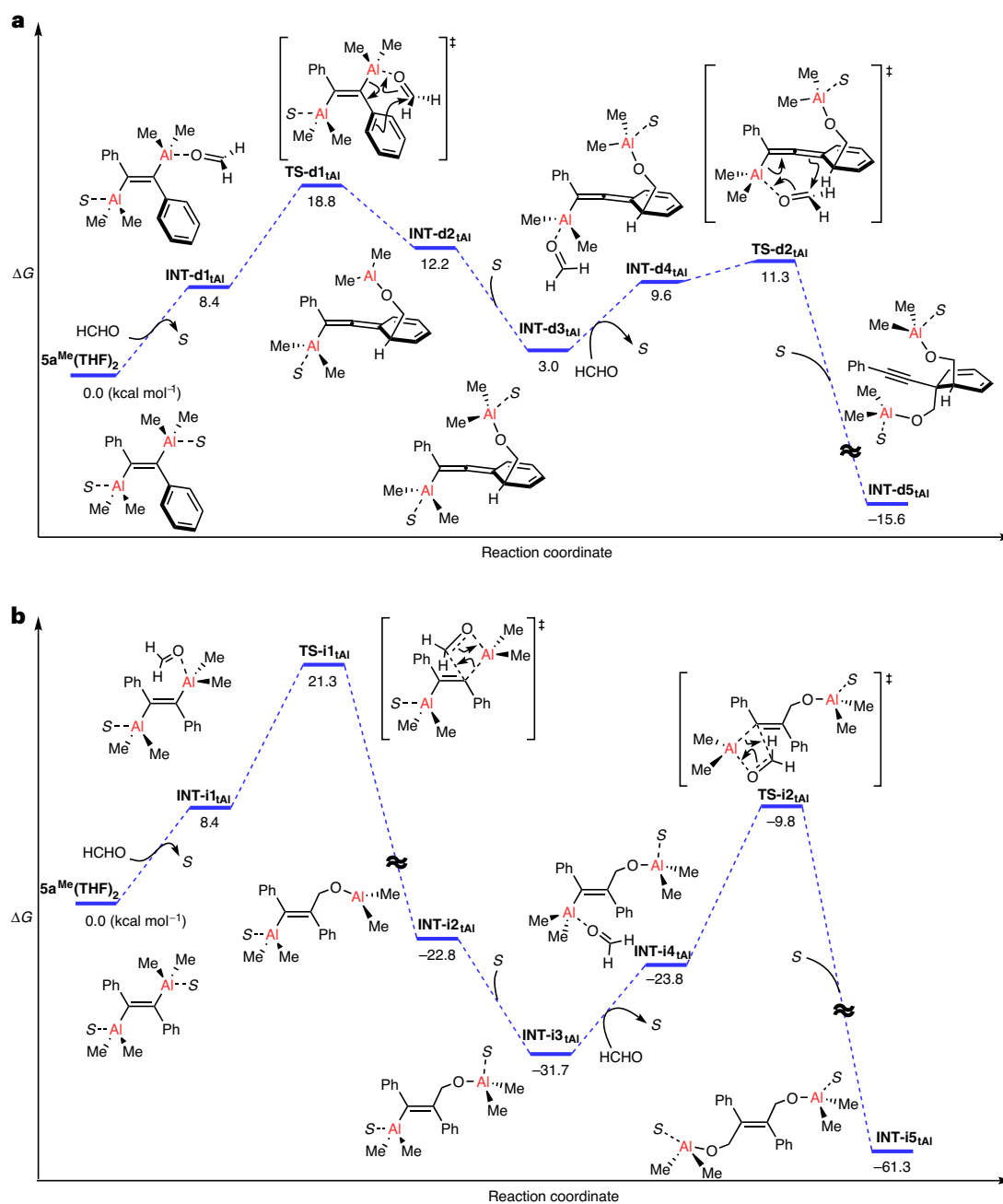


**Fig. 5** | DFT calculations for the reaction of  $5a^{Me}$  with formaldehyde. **a**, Calculated free energy diagram for the dearomatization reaction of  $5a^{Me}(THF)_2$  with two molecules of formaldehyde. **b**, Calculated free energy diagram for the ipso-hydroxymethylation reaction of  $5a^{Me}(THF)_2$  with two molecules of

formaldehyde. S in this figure represents a THF solvent molecule. Free energies were calculated at the level of  $\omega$ B97X-D/def2-TZVPP/SMD(THF)// $\omega$ B97X-D/def2-SVP/SMD(THF) at 333.15 K.

Further exploration of the synthesis and utility of 1,2-dimetalloalkenes is ongoing in our laboratory.

## Methods

### General procedure for synthesis of 1,2-diborylalkenes 3

See Fig. 2a. An oven-dried 20 ml Schlenk tube was charged with alkyne **1** (1.0 mmol), <sup>n</sup>PentMgBr (1.0 M in THF, 2.0 ml, 2.0 mmol) and THF (2.0 ml). After cooling the mixture to 0 °C, sodium dispersion (10 M, 0.20 ml, 2.0 mmol) was added dropwise over 30 s to the tube, and the resulting suspension was stirred at 0 °C for 30 min. After the addition of <sup>i</sup>PrOBpin (1.2 ml, 6.0 mmol) to the tube, the reaction mixture was warmed to 60 °C and stirred at the same temperature for an additional 2 h.

After cooling the mixture to room temperature, aqueous HCl (2 M, 2 ml) and H<sub>2</sub>O (2 ml) were added to the tube, and the resulting biphasic solution was extracted with Et<sub>2</sub>O (4 ml × 3). The combined organic layer was dried over Na<sub>2</sub>SO<sub>4</sub>, filtered and concentrated under reduced pressure. Purification of the residue by column chromatography on silica gel (eluent: hexane/EtOAc) provided **3**.

### General procedure for copper-catalysed trans-difunctionalization of alkynes 1

See Fig. 2c. An oven-dried 20 ml Schlenk tube was charged with alkyne **1** (1.0 mmol), <sup>n</sup>PentMgBr (1.0 M in THF, 2.0 ml, 2.0 mmol) and THF (2.0 ml). After cooling the mixture to 0 °C, sodium dispersion (10 M,



0.20 ml, 2.0 mmol) was added dropwise over 30 s to the tube, and the resulting suspension was stirred at 0 °C for 30 min. After the addition of CuCN·2LiCl (1.0 M in THF, 0.10 ml, 0.10 mmol) and an electrophile (4.0 mmol) to the tube, the reaction mixture was allowed to warm to room temperature and stirred for an additional 1 h. The reaction was then quenched by the addition of aqueous HCl (2 M, 2 ml) and H<sub>2</sub>O (2 ml), and the resulting biphasic solution was extracted with Et<sub>2</sub>O (4 ml × 3). The combined organic layer was dried over Na<sub>2</sub>SO<sub>4</sub>, filtered and concentrated under reduced pressure. Purification of the residue by column chromatography on silica gel (eluent: hexane/EtOAc) provided **4**. If necessary, further purification was done by gel permeation chromatography.

### General procedure for synthesis of dearomatized diols **6**

See Fig. 3b. An oven-dried 20 ml Schlenk tube was charged with alkyne **1** (1.0 mmol), Me<sub>2</sub>AlCl (1.0 M in hexane, 2.0 ml, 2.0 mmol) and 4-MeTHP (6.0 ml). After cooling the mixture to -78 °C, sodium dispersion (10 M, 0.22 ml, 2.2 mmol) was added dropwise over 30 s to the tube, and the resulting suspension was stirred at -78 °C for 30 min. After the addition of paraformaldehyde (4.0 mmol) to the tube, the reaction mixture was allowed to warm to room temperature over 10 min and then stirred at 60 °C for an additional 1 h. After cooling the mixture to room temperature, the reaction was quenched by the addition of aqueous HCl (2 M, 3.5 ml), and the resulting biphasic solution was extracted with Et<sub>2</sub>O (4 ml × 3). The combined organic layer was dried over Na<sub>2</sub>SO<sub>4</sub>, filtered and concentrated under reduced pressure. Purification of the residue by column chromatography on silica gel (eluent: hexane/EtOAc) provided **6**.

### Data availability

Crystallographic data for the structures reported in this article have been deposited at the Cambridge Crystallographic Data Centre, under deposition numbers CCDC 2167281 (**2a**<sup>IPr</sup>(THF)<sub>4</sub>), CCDC 2167282 (**5a**<sup>Et</sup>(THF)<sub>2</sub>), CCDC 2167622 (**5a**<sup>Et-Cl</sup>(THF)<sub>2</sub>) and CCDC 2167689 (**8**). Copies of the data can be obtained free of charge via <https://www.ccdc.cam.ac.uk/structures/>. The data supporting the findings of this study are available within the Article and its Supplementary Information.

### References

- Schlosser, M. (ed.) *Organometallics in Synthesis: A Manual* (Wiley, 2002).
- Harutyunyan, S. R., den Hartog, T., Geurts, K., Minnaard, A. J. & Feringa, B. L. Catalytic asymmetric conjugate addition and allylic alkylation with Grignard reagents. *Chem. Rev.* **108**, 2824–2852 (2008).
- Knappke, C. E. I. & von Wangelin, A. J. 35 years of palladium-catalyzed cross-coupling with Grignard reagents: how far have we come? *Chem. Soc. Rev.* **40**, 4948–4962 (2011).
- Knochel, P. et al. Highly functionalized organomagnesium reagents prepared through halogen–metal exchange. *Angew. Chem. Int. Ed.* **42**, 4302–4320 (2003).
- Boudier, A., Bromm, L. O., Lotz, M. & Knochel, P. New applications of polyfunctional organometallic compounds in organic synthesis. *Angew. Chem. Int. Ed.* **39**, 4414–4435 (2000).
- Hevia, E. Towards a paradigm shift in polar organometallic chemistry. *Chimia* **74**, 681–688 (2020).
- Marek, I. Enantioselective carbometallation of unactivated olefins. *J. Chem. Soc. Perkin* **1** **1999**, 535–544 (1999).
- Flynn, A. B. & Ogilvie, W. W. Stereocontrolled synthesis of tetrasubstituted olefins. *Chem. Rev.* **107**, 4698–4745 (2007).
- Müller, D. S. & Marek, I. Copper mediated carbometallation reactions. *Chem. Soc. Rev.* **45**, 4552–4566 (2016).
- Murakami, K. & Yorimitsu, H. Recent advances in transition-metal-catalyzed intermolecular carbomagnesiation and carbozincation. *Beilstein J. Org. Chem.* **9**, 278–302 (2013).
- Wei, D. & Darcel, C. Iron catalysis in reduction and hydrometalation reactions. *Chem. Rev.* **119**, 2550–2610 (2019).
- Fürstner, A. *trans*-Hydrogenation, *gem*-hydrogenation, and *trans*-hydrometalation of alkynes: an interim report on an unorthodox reactivity paradigm. *J. Am. Chem. Soc.* **141**, 11–24 (2019).
- Levin, G., Jagur-Grodzinski, J. & Szwarc, M. Chemistry of radical anions and dianions of diphenylacetylene. *J. Am. Chem. Soc.* **92**, 2268–2275 (1970).
- Dange, D. et al. Acyclic 1,2-dimagnesioethanes/-ethene derived from magnesium(I) compounds: multipurpose reagents for organometallic synthesis. *Chem. Sci.* **10**, 3208–3216 (2019).
- Zhao, Y., Liu, Y., Lei, Y., Wu, B. & Yang, X.-J. Activation of alkynes by an α-diimine-stabilized Al–Al-bonded compound: insertion into the Al–Al bond or cycloaddition to AlN<sub>2</sub>C<sub>2</sub> rings. *Chem. Commun.* **49**, 4546–4548 (2013).
- Hofmann, A. et al. Dialumination of unsaturated species with a reactive bis(cyclopentadienyl)dialane. *Chem. Commun.* **54**, 1639–1642 (2018).
- Chlupatý, T., Turek, J., De Proft, F., Růžičková, Z. & Růžička, A. Addition of in situ reduced amidinatomethylaluminum chloride to acetylenes. *Dalton Trans.* **44**, 17462–17466 (2015).
- Cui, C. et al. Facile synthesis of cyclopropene analogues of aluminum and an aluminum pinacolate, and the reactivity of LA[η<sup>2</sup>-C<sub>2</sub>(SiMe<sub>3</sub>)<sub>2</sub>] toward unsaturated molecules (L=HC[(CMe)(NAr)]<sub>2</sub>, Ar=2,6-*i*-Pr<sub>2</sub>C<sub>6</sub>H<sub>3</sub>). *J. Am. Chem. Soc.* **123**, 9091–9098 (2001).
- Schlenk, W. & Bergmann, E. Forschungen auf dem gebiete der alkaliorganischen verbindungen. I. Über produkte der addition von alkalimetall an mehrfache kohlenstoff-kohlenstoff-bindungen. *Justus Liebigs Ann. Chem.* **463**, 1–97 (1928).
- Smith, L. I. & Hoehn, H. H. The reaction between lithium and diphenylacetylene. *J. Am. Chem. Soc.* **63**, 1184–1187 (1941).
- Engler, T. A., Combrink, K. D. & Ray, J. E. An efficient method for the synthesis of 1-arylalkynes. *Synth. Commun.* **19**, 1735–1744 (1989).
- Spencer, J. T. & Grimes, R. N. Organotransition-metal metallacarboranes. 9. *nido*-2,3-Dibenzyl-2,3-dicarbahexaborane(8) [(PhCH<sub>2</sub>)<sub>2</sub>C<sub>2</sub>B<sub>4</sub>H<sub>6</sub>], a versatile multifunctional *nido*-carborane: iron–polyarene sandwich compounds and chromium tricarbonyl π-complexes. *Organometallics* **6**, 328–335 (1987).
- Al-jumaili, M. A. & Woodward, S. Syntheses of 7-substituted anthra[2,3-*b*]thiophene derivatives and naphtho[2,3-*b*:6,7-*b'*]dithiophene. *J. Org. Chem.* **83**, 11437–11445 (2018).
- De, P. B., Asako, S. & Ilies, L. Recent advances in the use of sodium dispersion for organic synthesis. *Synthesis* **53**, 3180–3192 (2021).
- An, J., Work, D. N., Kenyon, C. & Procter, D. J. Evaluating a sodium dispersion reagent for the Bouveault–Blanc reduction of esters. *J. Org. Chem.* **79**, 6743–6747 (2014).
- Asako, S., Nakajima, H. & Takai, K. Organosodium compounds for catalytic cross-coupling. *Nat. Catal.* **2**, 297–303 (2019).
- Peters, B. K. et al. Scalable and safe synthetic organic electroreduction inspired by Li-ion battery chemistry. *Science* **363**, 838–845 (2019).
- Burrows, J., Kamo, S. & Koide, K. Scalable Birch reduction with lithium and ethylenediamine in tetrahydrofuran. *Science* **374**, 741–746 (2021).
- Takahashi, F., Nogi, K., Sasamori, T. & Yorimitsu, H. Diborative reduction of alkynes to 1,2-diboryl-1,2-dimetalloalkanes: its application for the synthesis of diverse 1,2-bis(boronate)s. *Org. Lett.* **21**, 4739–4744 (2019).
- Ito, S., Fukazawa, M., Takahashi, F., Nogi, K. & Yorimitsu, H. Sodium-metal-promoted reductive 1,2-*syn*-diboration of alkynes with reduction-resistant trimethoxyborane. *Bull. Chem. Soc. Jpn.* **93**, 1171–1179 (2020).

31. Fukazawa, M., Takahashi, F., Nogi, K., Sasamori, K. & Yorimitsu, H. Reductive difunctionalization of aryl alkenes with sodium metal and reduction-resistant alkoxy-substituted electrophiles. *Org. Lett.* **22**, 2303–2307 (2020).
32. Cheng, Y.-Z., Feng, Z., Zhang, X. & You, S.-L. Visible-light induced dearomatization reactions. *Chem. Soc. Rev.* **51**, 2145–2170 (2022).
33. Sharma, U. K., Ranjan, P., Van der Eyken, E. V. & You, S.-L. Sequential and direct multicomponent reaction (MCR)-based dearomatization strategies. *Chem. Soc. Rev.* **49**, 8721–8748 (2020).
34. Huck, C. J. & Sarlah, D. Shaping molecular landscapes: recent advances, opportunities, and challenges in dearomatization. *Chem* **6**, 1589–1603 (2020).
35. Wertjes, W. C., Southgate, E. H. & Sarlah, D. Recent advances in chemical dearomatization of nonactivated arenes. *Chem. Soc. Rev.* **47**, 7996–8017 (2018).
36. Zheng, C. & You, S.-L. Catalytic asymmetric dearomatization by transition-metal catalysis: a method for transformations of aromatic compounds. *Chem* **1**, 830–857 (2016).
37. Zhuo, C.-X., Zhang, W. & You, S.-L. Catalytic asymmetric dearomatization reaction. *Angew. Chem. Int. Ed.* **51**, 12662–12686 (2012).
38. Roche, S. P. & Porco, J. A. Jr. Dearomatization strategies in the synthesis of complex natural products. *Angew. Chem. Int. Ed.* **50**, 4068–4093 (2011).
39. Rieke, R. D. Preparation of highly reactive metal powders and their use in organic and organometallic synthesis. *Acc. Chem. Res.* **10**, 301–306 (1977).
40. Kojima, C., Lee, K.-H., Lin, Z. & Yamashita, M. Direct and base-catalyzed diboration of alkynes using the unsymmetrical diborane(4), pinB-BMes<sub>2</sub>. *J. Am. Chem. Soc.* **138**, 6662–6669 (2016).
41. Yoshimura, A. et al. Photoinduced metal-free diboration of alkynes in the presence of organophosphine catalysts. *Tetrahedron* **72**, 7832–7838 (2016).
42. Nagashima, Y., Hirano, K., Takita, R. & Uchiyama, M. *Trans*-diborylation of alkynes: *pseudo*-intramolecular strategy utilizing a propargylic alcohol unit. *J. Am. Chem. Soc.* **136**, 8532–8535 (2014).
43. Nagao, K., Ohmiya, H. & Sawamura, M. *Anti*-selective vicinal silaboration and diboration of alkynoates through phosphine organocatalysis. *Org. Lett.* **17**, 1304–1307 (2015).
44. Ohmura, T., Morimasa, Y. & Suginome, M. 4,4'-Bipyridine-catalyzed stereoselective *trans*-diboration of acetylenedicarboxylates to 2,3-diborylfumarates. *Chem. Lett.* **46**, 1793–1796 (2017).
45. Knochel, P., Yeh, M. C. P., Berk, S. C. & Talbert, J. Synthesis and reactivity toward acyl chlorides and enones of the new highly functionalized copper reagents RCu(CN)ZnI. *J. Org. Chem.* **53**, 2390–2392 (1988).
46. Minami, Y., Shiraishi, Y., Yamada, K. & Hiyama, T. Palladium-catalyzed cycloaddition of alkynyl aryl ethers with internal alkynes via selective *ortho* C–H activation. *J. Am. Chem. Soc.* **134**, 6124–6127 (2012).
47. Chernyak, N. & Gevorgyan, V. Exclusive 5-*exo-dig* hydroarylation of *o*-alkynyl biaryls proceeding via C–H activation pathway. *J. Am. Chem. Soc.* **130**, 5636–5637 (2008).
48. Alcaide, B., Almendros, P. & Carrascosa, R. Gold-catalyzed direct cycloketalization of acetonide-tethered alkynes in the presence of water. *Tetrahedron* **68**, 9391–9396 (2012).
49. Baran, A. & Balci, M. Stereoselective synthesis of bishomo-inositols as glycosidase inhibitors. *J. Org. Chem.* **74**, 88–95 (2009).
50. Ohno, T., Ozaki, M., Inagaki, A., Hirashima, T. & Nishiguchi, I. Synthesis of 1,2-disubstituted benzenes and biphenyls from phthalic acids through electroreduction followed by electrocyclic reaction with alkynes. *Tetrahedron Lett.* **34**, 2629–2632 (1993).
51. Lehmkuhl, H., Čuljković, J. & Nehl, H. Reaktionen von Trialkylaluminium mit Alkalimetallen oder Magnesium und elektronenaffinen Olefinen. *Liebigs Ann. Chem.* **1973**, 666–691 (1973).
52. Benkeser, R. A. & Snyder, D. C. Mechanism of the reaction between benzylmagnesium chloride and carbonyl compounds. A detailed study with formaldehyde. *J. Org. Chem.* **47**, 1243–1249 (1982).
53. Eisch, J. J. & Fichter, K. C. Kinetic control and locoselectivity in the electrophilic cleavage of allylic aluminum compounds: reactions of acenaphthenylaluminum reagents with carbonyl substrates. *J. Org. Chem.* **49**, 4631–4639 (1984).
54. Fernández, I. & Bickelhaupt, F. M. The activation strain model and molecular orbital theory: understanding and designing chemical reactions. *Chem. Soc. Rev.* **43**, 4953–4967 (2014).
55. Bickelhaupt, F. M. & Houk, K. N. Analyzing reaction rates with the distortion/interaction-activation strain model. *Angew. Chem. Int. Ed.* **56**, 10070–10086 (2017).

## Acknowledgements

This work was supported by JST CREST grant number JPMJCR19R4 and by JSPS KAKENHI grant number JP19H00895 to H.Y. F.T. acknowledges a JSPS Predoctoral Fellowship (JSPS KAKENHI grant number JP20J22814). H.Y. thanks The Asahi Glass Foundation for financial support. We thank Kobelco Eco-Solutions for providing the sodium dispersion. F.T. thanks H. Saito for insightful discussions on the computational chemistry. We also thank H. Kawaguchi and Y. Ishida for conducting elemental analyses of **2a**<sup>Pr</sup>(THF)<sub>4</sub> and **5a**<sup>Et</sup>(THF)<sub>2</sub> at the Tokyo Institute of Technology.

## Author contributions

F.T. and H.Y. conceived of and designed the project. F.T. performed all the experiments and computational chemistry, except for the X-ray crystallography. T.K. synthesized metal complexes and performed the X-ray crystallography. All authors contributed to the writing and editing of the manuscript.

## Competing interests

The authors declare no competing interests.

## Additional information

**Supplementary information** The online version contains supplementary material available at <https://doi.org/10.1038/s44160-022-00189-z>.

**Correspondence and requests for materials** should be addressed to Hideki Yorimitsu.

**Peer review information** *Nature Synthesis* thanks the anonymous reviewers for their contribution to the peer review of this work. Primary handling editor: Thomas West, in collaboration with the *Nature Synthesis* team.

**Reprints and permissions information** is available at [www.nature.com/reprints](http://www.nature.com/reprints).

**Publisher's note** Springer Nature remains neutral with regard to jurisdictional claims in published maps and institutional affiliations.

**Open Access** This article is licensed under a Creative Commons Attribution 4.0 International License, which permits use, sharing, adaptation, distribution and reproduction in any medium or format, as long as you give appropriate credit to the original author(s) and the source, provide a link to the Creative Commons license, and indicate

if changes were made. The images or other third party material in this article are included in the article's Creative Commons license, unless indicated otherwise in a credit line to the material. If material is not included in the article's Creative Commons license and your intended use is not permitted by statutory regulation or exceeds the permitted

use, you will need to obtain permission directly from the copyright holder. To view a copy of this license, visit <http://creativecommons.org/licenses/by/4.0/>.

© The Author(s) 2023